Title	Electro -absorptive and electro -optic quantum well modulators using surface acoustic wave
Author(s)	Choy, WCH; Weiss, BL; Li, EH
Citation	Proceedings Of Spie - The International Society For Optical Engineering, 1998, v. 3278, p. 73-83
Issued Date	1998
URL	http://hdl.handle.net/10722/46083
Rights	Creative Commons: Attribution 3.0 Hong Kong License

Electro -absorptive and electro -optic quantum well modulators using surface acoustic wave

Wallace C. H. Choy[a], Bernard L. Weiss[a], and E. Herbert Li[b]

[a] School of Electronic Engineering, Information Technology and Mathematics, University of Surrey, Guildford, Surrey, GU2 5XH, UK

[b] Department of Electrical & Electronic Engineering, University of Hong Kong, Pokfulam Road, Hong Kong

ABSTRACT

The characteristics of $Al_{0.3}Ga_{0.7}As/GaAs$ QW acousto-absorption and acousto-optic modulators using the interaction between Surface Acoustic Wave (SAW) and quantum well (QW) optical waveguide structures are analyzed here theoretically. The QW structures are optimized by maximizing the optical confinement of modal field in the active region and the piezoelectric effect of SAW on QWs. The electric field induced by SAW reduces non-uniformly in depth, which limits in the development of high efficiency modulators, especially for devices with a large number of QWs in the active region. We present the results of the analysis of a range of QW SQW modulators using between one and 25 QWs in the active region. For devices with thin active regions, the QW structures are designed so that at the top surface strong SAW effects can be obtained while for the 25 periods structure, the QWs located at a depth of 2/3 SAW wavelength in order to obtain an uniform SAW induced electric field. The results show that the single and five QW devices are suitable for absorptive modulation and optical modulation respectively while the 25-QW modulators can shorten the modulation interaction length and thus increase modulation bandwidth. The effective index change of these devices are at least 10 times larger than the conventional surface acoustic wave devices. These results make the quantum-well modulators more attractive for the development of acousto-optic device applications.

Keywords: surface acoustic wave, AlGaAs/GaAs quantum well, acousto-optic devices, modulators, piezoelectric effect of SAW, optical confinement of SAW devices.

1. INTRODUCTION

Among the various applications of Surface Acoustic Wave (SAW), a number of acousto-optical signal processing functions including modulation,[1] beam deflection,[2] tunable filtering[3] and spectrum analysis[4] have been developed. Most of these applications use the change of refractive index induced by the elasto-optic and electro-optic effects of a SAW. Recently, the studies of absorptive modulation generated by SAW have also been initiated[5] ,which indicate that both the absorption change and refractive index change induced by SAW are attractive in modulation devices. SAWs have been widely investigated in piezoelectric bulk materials included $LiNbO_3$ and GaAs while their use in QW structures has not been studied in detailed. In comparison to bulk materials, QWs are attractive for their excitonic optical properties[6,7] and thus are useful for electro-absorptive and electro-optic modulators[8,9] as with the quantum-confined Stark effect (QCSE)

The electric field induced by SAW reduce non-uniformly with depth,[3] which is an obstacle in the development of high efficiency modulators typically with a large number of QWs in the active region. Moreover, the penetration depth of SAW is usually one SAW wavelength (λ_{SAW}) deep. Here we analyzing single QW, 5-period QW and 25-period QW SAW modulators, all of which are within one λ_{SAW} from the surface.

In this paper, a theoretically analysis of the waveguide type 100Å/100Å $Al_{0.3}Ga_{0.7}As/GaAs$ optical and absorptive modulators by using SAW is presented. This study addresses the non-linear SAW effects on the QWs absorption coefficient and refractive index, the effect of optical confinement to the modulation efficiency, and the design and optimization of a 1, 5 and 25-period QW modulators. The comparison between these three structures are also made so that the results can be used as a guideline to develop SAW-QW modulators.

2. MODELING THE SAW QUANTUM WELL MODULATORS

The waveguide type absorptive and optical modulators have an identical device structure and are shown schematically in Fig. 1. Starting from the substrate, the layers are an AlGaAs cladding, a stack of 100Å $Al_{0.3}Ga_{0.7}As$ barriers and 100Å thick GaAs wells which serve as the active region of the device, and a top cladding AlGaAs layer. An interdigital transducer is fabricated on the top surface for the generation of the SAWs. In order to investigate the optical

and absorptive modulators, the SAW propagation and its piezo-electric and elasto-electric effects are modeled followed by their effects on the QW subband structure. The optical properties, including absorption coefficient and refractive index of these structures with the effects of excitons, are then determined. In order to take into account the interaction of the optical waveguide mode field with the QW structure, a one dimensional Maxwell's equation is solved analytically. Subsequently, the change of both the effective absorption coefficient and the effective refractive index are calculated. Various performance parameters are then determined to characterize the modulation performance.

A.   SAW Perturbation on Quantum Well structures

The propagation of SAW is described by two equations. One is the motion equation of particles in elastic medium, which is given as:

$$\frac{\partial T_{ij}}{\partial x_j} = \rho \frac{\partial^2 u_i}{\partial t^2},$$

(1)

where T_{ij}, u_i and x_j are a components of the stress tensor, the particle displacement and the spatial direction, respectively, with the indices i and j labelling the spatial directions and summation over repeated indices has been implied. Equation (2) describes the electromagnetic wave properties of SAW, in which Maxwell's equations govern the electric fields and electric displacements of SAW. Under a quasi-static approximation, the electric displacement equation in a medium of no free charges is given as:

$$\frac{\partial D_i}{\partial x_j} = 0$$

(2)

where D is the electric displacement field. The method used to solve these two equations for a multilayered structures is described in ref. 10 and 11. In order to obtain a high electromechanical coupling constant (to produce a large SAW amplitude) for structures such as GaAs and AlGaAs, the growth direction of the QW is <100> and the SAW propagates along the <110>.[10]

A typical perturbation method is used to evaluate the SAW effects in the QW subband structure. The SAW induces both strain and electric field in the AlGaAs/GaAs heterostructure, which is a piezoelectric material. However the induced strains are small (<0.1%) and are not large enough to modify the QW potential profile to produce a useful change of the semiconductor material bandgap.[12] Consequently, only the SAW-induced electric field is considered as an extra linear perturbation term to the QW potential profile. The transverse electric (TE) and transverse magnetic (TM) polarization dependent refractive index and absorption coefficients, including the contributions from the exciton, are determined.   Details of the refractive index and absorption coefficient calculations can be found in refs. 12 and 14 respectively. In our model, the refractive index is averaged for each QW period and the absorption coefficient is produced by the wells.

B.   Optical Properties of the SAW Modulator

When an optical field propagates in the devices, only that portion which interacts with the QWs will be modulated by the SAW effect. In order to calculate the optical properties (including the effective absorption coefficient and refractive index) of an acousto-optic QW modulator structure, a multilayer planar waveguide model is developed from our previous model[15] using the transfer matrix method. From this calculation, the modal field profiles and the propagation constants are obtained for the determination of the effective absorption coefficient and effective refractive index, respectively.

The effective absorption coefficient, α_{eff}, is given by :

$$\alpha_{eff} = \left. \int_{\substack{\text{the wells within} \\ \text{the active region}}} \alpha\,(z)\varphi\,(z)\varphi^*(z)dz \middle/ \int_{\substack{\text{the entire cover range} \\ \text{of the guiding field}}} \varphi\,(z)\ \varphi^*(z)dz \right. ,$$

(3)

where $\varphi(z)$ is the guiding optical field and $\alpha(z)$ is the material absorption coefficient of the QW structure. Since the amplitude of SAW varies with penetration depth, α is z dependent. Equation (3) shows that α_{eff} is determined by the fraction of the optical field intensity $\varphi(z)\varphi^*(z)$ within the wells of active region. The change of effective absorption coefficient $\Delta\alpha_{eff}$ of the device is calculated using :

$$\Delta\alpha_{eff} = \alpha_{eff}(SAW) - \alpha_{eff}(no\ SAW),$$

(4)

where $\alpha_{eff}(SAW)$ and $\alpha_{eff}(no\ SAW)$ are the effective absorption coefficients with and without SAW-induced electric field respectively.

The effective refractive index of the structure, n_{eff}, is determined by solving Maxwell's equations for the waveguide using the material refractive indices. The change of the effective refractive index, Δn_{eff}, is calculated using :

$$\Delta n_{eff} = n_{eff}(SAW) - n_{eff}(no\ SAW),$$
(5)

where $n_{eff}(SAW)$ and $n_{eff}(no\ SAW)$ are the effective refractive indices with and without SAW-induced electric field respectively.

C.   Modulator Performance

The important performance characteristics of the modulators are the modulation depth η for phase or diffraction modulation, the contrast ratio CR for absorptive modulation, optical confinement factor Γ, the chirp parameter β_{mod} and the absorption loss α_{loss} for both modulations.

The modulation depth η indicates the efficiency of modulation due to the change of the effective index, such as diffraction and phase modulation, is given by :

$$\eta = \sin^2(\Delta\phi / 2),$$
(6)

where $\Delta\phi = 2\pi l \Delta n_{eff} / \lambda_{op}$ is the phase change, l is the SAW aperture and λ_{op} is the operating optical wavelength. The SAW aperture for π phase change is commonly used to measure the phase modulation, the smaller the SAW aperture the larger the phase modulation can be obtained.

The contrast ratio CR is defined as the ratio of the light intensity with and without an SAW and is given by :

$$CR(dB) = 10\log\left(\frac{\exp(-\alpha_{eff}(ON)l)}{\exp(-\alpha_{eff}(OFF)l)}\right),$$
(7)

where $\alpha_{eff}(ON)$ and $\alpha_{eff}(OFF)$ are the effective absorptions in the ON-state (no SAW-induced electric field) and the OFF-state (under SAW-induced electric field), respectively.

The static chirp parameter β_{mod} is given by :

$$\beta_{mod} = (4\pi\ \Delta n_{eff}) / (\lambda_{op}\ \Delta\alpha_{eff})$$
(8)

where Δn_{eff} and $\Delta\alpha_{eff}$ are the change in the effective refractive index and the change in the effective absorption respectively. Equation (8) shows that β_{mod} can be considered top be a measure of the ratio of the optical (refractive index) modulation strength to the optical intensity (absorption coefficient) modulation strength due to the SAW-induced electric field. Typical electro-optical (refractive index) and electro-absorptive types of modulator require chirp parameters of larger than 10 and less than 1, respectively. [16]

The optical confinement factor Γ is determined using

$$\Gamma = \left.\int_{\substack{\text{the core region of} \\ \text{the waveguide device}}} \varphi\ (z)\ \varphi^*(z)dz \middle/ \int_{\substack{\text{the entire cover range} \\ \text{of a guiding field}}} \varphi\ (z)\ \varphi^*(z)dz \right.,$$
(9)

where $\varphi(z)$ is the modal electric field profile in the device structure and z is the growth direction of QW. This Γ parameter indicates the portion of the optical power overlap with the core region, which consists of the QW active region and the AlGaAs buffer regions above and below the QWs, which are surrounded by AlGaAs cladding layers above and below the core region. Therefore, an efficient modulator requires a large value of Γ. High performance modulators also requires low α_{loss}, which is a measure of the insertion loss of the device. For phase modulation, α_{loss} is defined as α_{eff} without the SAW effect while, for absorptive modulator, α_{loss} is defined as the ON-state α_{eff}.

3. RESULTS AND DISCUSSIONS

The three QW structures considered here contain 1, 5 and 25 periods of an $100\text{Å}/100\text{Å}$ $Al_{0.3}Ga_{0.7}As/GaAs$ QW structure. They are used as an active region of the acousto -absorptive and -optic modulators. It should be noted that a high performance absorptive modulator requires a high CR, a low optical modulation (and thus low β_{mod}), and a low α_{loss}. On the other hand, a good electro-optic modulator requires a high η, a large phase change, a low absorption change (and thus high β_{mod}), a short SAW aperture for π phase change and a low α_{loss}.

The effects of SAW on the QWs are first investigated. Through the understanding of optical guiding and interaction between the modal field and active region, a five period and a single QW modulator are then analyzed. In order to enhance the modulation efficiency and to reduce the SAW aperture (modulation length), an optimised QW modulator structure containing 25 QWs is designed and its performance are also considered here.

A.   SAW Effects in QW Structures

The effects of SAW, with power and wavelength of 10mW and 2μm respectively, on the optical properties of 25-period of QWs structures on top of a thick $Al_{0.5}Ga_{0.5}As$ lower cladding layer are considered here. The QW potential profiles are tilted by the SAW induced potential, as shown in Fig. 2. It can be observed that the slope of the QW potential profile reduces gradually and eventually slightly increases in the deeper QWs. The wavefunctions of the fundamental states over these 25 QWs are localized in the wells without significant tunnelling between adjacent wells. The corresponding absorption spectra of this 25-QW structure is shown in Fig. 3. The quantum confined Stark shift reduces with depth starting from the first QW since the gradient of QW potential profile reduces. The Stark shift between the 5th and 25th QW is so small that the exciton edges is at almost the same wavelength as that of the QW exciton band edge without any SAW effect. Consequently, only the first 5 QWs (thickness equivalent to a depth of 0.05 λ_{SAW}) are suitable for use as a QCSE modulator.

B.   5-Period QW Modulator

To develop the 5-QW structure as optical and absorptive modulators, the SAW effect has to be enhanced and the modal optical field has to be confined to these 5 QWs for optimizing the modulation efficiency. The results show that the SAW-induced electric field can be increased by reducing the number of QWs from 25 to 5. This improvement can be enhanced further by increasing the Al composition of the lower cladding layer from $Al_{0.5}Ga_{0.5}As$ to AlAs. However, since the waveguide core region of 0.11μm (5-QW) is too thin to support any guiding modes, an extra buffer layer of $Al_{0.5}Ga_{0.5}As$ is inserted between the QWs and lower cladding layer. By increasing the thickness of this buffer layer from 0 to 0.04μm, the first guided mode is obtained. Therefore, the optimized structure contains a GaAs substrate, a 2μm AlAs cladding layer, a 0.04μm $Al_{0.5}Ga_{0.5}As$ buffer layer with 5 QWs on top. The SAW power and λ_{SAW} are 10mW and 2μm respectively. As compared to the previous 25-QW structure, the optical confinement of the modal field in the top five QWs (thickness equivalent to 0.05 λ_{SAW}) improves by more than 40 times from less than 0.01 to 0.4 in the optimized structure which results in a higher modulation efficiency.

Table 1. Modulation properties of the 5 QWs modulator. The SAW aperture is 500μm.

λ_{op} (μm)	α_{loss} (cm^{-1})	$\Delta\alpha_{eff}$ (cm^{-1})	Δn_{eff} (10^{-2})	CR (dB)	β_{mod}
		absorptive modulation			
0.860	225.0	436.7	−1.27	21.8	−4.24
0.862	155.7	423.8	−6.36	21.2	−21.88
0.863	133.2	437.6	−4.01	21.9	−1.35
0.864	115.7	427.5	−0.50	21.4	−0.50
8.866	90.4	293.7	−0.45	14.6	−0.45

λ_{op} (μm)	α_{loss} (cm^{-1})	$\Delta\alpha_{eff}$ (cm^{-1})	n_{eff} (SAW)	n_{eff} (no SAW)	$\Delta\phi$ (rad.)	η	l for $\Delta\phi=\pi$	β_{mod}
			phase modulation					
0.876	39.9	43.3	3.07548	3.07529	0.68	0.11	2305	0.62
0.878	35.6	49.7	3.07317	3.07246	2.54	0.91	618	2.04
0.880	32.1	16.6	0.07059	3.06983	2.71	0.95	579	6.54
0.881	30.5	7.3	3.06918	3.06859	2.10	0.75	746	11.5
0.882	29.1	2.0	3.06783	3.06739	1.56	0.50	1002	31.3

The absorption modulator is selected to operate at the wavelength of the HH exciton peak in the presence of a SAW. The TE mode absorption coefficient of the 5-QW structure is shown in Fig. 4. Although the exciton band edges of these 5 QWs do not coincide due to the decay of the SAW-induced electric field with depth, the magnitude of quantum confined Stark shift of each of these QWs increases by comparing the 1st QW and the 5th QW to that of the previous 25-QW structure. This implies that the optimised structure is more practical for device applications. The electro-optic and electro-absorptive modulators of the 5-QW device are given in Table 1. In order to have a lower α_{loss}, λ_{op} should be kept away (≥ 0.86μm) from the exciton absorption edge without the SAW effect. λ_{op} is selected to be 0.864 μm for an optimised absorptive modulation. For a SAW aperture of 500 μm, the CR, α_{loss} and β_{mod} are 21.4 dB, 427.5 cm^{-1} and −0.5

respectively. β_{mod} is negative at this wavelength, so that frequency compression of the optical source is possible which makes this modulator attractive.

For optical modulation, the change of refractive index spectra are shown in Fig. 5. β_{mod} is > 10 , which is the requirement for a good phase modulator, for λ_{op} above 0.881µm. The value of β_{mod} can be increased by operating at longer wavelength, although there is a smaller associated phase change as shown in Table 1. As a consequence, the selected operating wavelength λ_{op} is above 0.881 µm, at where $\Delta\phi$ is 2.1 radian and α_{loss} is only 7.3 cm^{-1}.

C.   Single QW Modulator

In order to improve the absorption modulation to obtain a higher CR and lower α_{loss}, as compared to the previous 5-QWs case, a single QW structure is used. In the previous 5-QW structure the mode field peaks at ~ 0.1µm and the thickness of the core region (including the buffer region) is the minimum thickness required to obtain a single mode operation. Consequently, the single QW structure is designed to put the QW at a depth of 0.1µm and the thickness of the core for the single QW device is similar to that of the 5-QW structure. This will result in a strong overlap between the mode field profile and the active region together with a well confined single optical mode. The structure of the single QW modulator is a GaAs substrate, 2µm AlAs lower cladding layer, 0.04µm $Al_{0.5}Ga_{0.5}As$ buffer region, 100Å/100Å $Al_{0.3}Ga_{0.7}As$/GaAs single QW, and 0.08 µm upper $Al_{0.5}Ga_{0.5}As$ cladding layer. The power of SAW and λ_{SAW} are the same as those for the 5QW structure.

Table 2. Modulation properties of the single QW modulator. The SAW aperture is 500 µm.

λ_{op} (µm)	α_{loss} (cm^{-1})	$\Delta\alpha_{eff}$ (cm^{-1})	Δn_{eff} (10^{-2})	CR (dB)	β_{mod}		
absorptive modulation							
0.859	71.6	356.8	−2.12	17.8	−0.87		
0.86	57.6	351.0	3.21	17.5	1.34		
0.861	47.4	112.5	4.02	10.6	2.77		
0.862	39.9	62.2	2.98	5.6	3.86		
0.863	34.2	36.2	2.05	3.1	4.80		
phase modulation							
λ_{op} (µm)	α_{loss} (cm^{-1})	$\Delta\alpha_{eff}$ (cm^{-1})	n_{eff} (SAW)	n_{eff} (no SAW)	$\Delta\phi$ (rad.)	η	l for $\Delta\phi=\pi$	β_{mod}
0.864	29.7	36.2	3.04840	3.04698	5.16	0.28	304	5.7
0.865	26.1	22.0	3.04644	3.04543	3.67	0.93	428	6.8
0.866	23.2	13.6	3.04462	3.04396	2.39	0.87	656	7.0
0.867	20.8	8.5	3.04287	3.04250	1.34	0.39	1171	6.3
0.868	18.8	5.2	3.04135	3.04109	0.94	0.21	1669	7.2
0.869	17.4	2.7	3.03994	3.03970	0.86	0.19	1810	12.9
0.870	15.7	1.5	3.03855	3.03833	0.79	0.15	1977	21.2

The absorption modulator properties are given in Table 2. For a SAW aperture of 500 µm, the CR is 17.8 dB and β_{mod} is −0.87 at a λ_{op} of 0.864 µm. This value of β_{mod} is negative so that frequency compression can be achieved. Although the Γ of this device reduces to 0.2, half that of the 5QW structure, the modulation performance, in terms of α_{loss} and CR, is better than the 5QW structure. The main reason is that, α_{loss} in the single QW device 71.6cm^{-1} which is only ~ 60% of that in the 5QW structure at for a λ_{op} between 0.862 and 0.866µm. For the same optical power loss, the CR of the single QW structure can be increased by more than seventeen times, i.e. ~124 dB, while that of 5-QW one is only 22.7 dB. In the single QW structure, only the QW contributes to α_{loss} and there is no absorption loss in the bulk AlGaAs cladding layers at such long λ_{op}. On the other hand, in the 5-QW case, due to the variation of the exciton edges of the 5 QWs, the 4th QW predominantly determines the absorption change of the optical field at the optimised λ_{op} = 0.864µm, while other QWs provide a weaker absorption change, as shown in Fig. 4. Moreover, at the optimized operating wavelength, all of the QWs provide the same amount of α_{loss} (115.7cm^{-1}) without any SAW induced effects. These effects explain why the single QW structure has a better modulation performance than the 5-QW structure.

A λ_{op} of 0.869µm is selected for the operating wavelength of the phase modulator since the optical modulation is larger in the region with β_{mod} > 10, as shown in Table 2. When λ_{op} is reduced to 0.866µm, a larger phase change of 2.39

radians can be obtained but β_{mod} is relative weak, 7. By comparing the modulation performance in terms of phase change, for the same power loss, this single QW device is 1.52 radians at the selected λ_{op}, which is weaker than that of the 5-QW structure at λ_{op} of 0.882 μm. Consequently, the 5-QW modulator provides a better phase modulation while the single QW structure is better for absorption modulation.

D.   25-Period QW Modulator

There are two important factors in the development of a SAW modulator with 25-period (~0.5μm) QW active region. Firstly, a linear SAW-induced potential over a depth of 0.5μm is required so that consistent exciton absorption edges can be obtained. Secondly, a large SAW potential gradient $\geq$ 50 kV/cm is required so that a large enough QCSE can be produced. As shown in Fig. 6, a more linear SAW-induced potential is obtained by increasing λ_{SAW} from 2μm (solid line) to 3μm (dot line). However, the SAW potential is too weak to provide the required QCSE. A 0.3 λ_{SAW} thick layer of ZnO deposited on the top surface of the AlGaAs/GaAs material structure may be used to enhance the SAW induced potential by a factor of 7.[17] A linear SAW potential, with gradient equivalent to an applied electric field of ~ 80kV/cm, can therefore be obtained at depths between 1.7μm to 2.8μm; a range greater than 0.5 μm.

The absorption spectra of QWs at different depths are shown in Fig. 7. The strength of the QCSE at depths ranging from 1.9μm (equivalent to a depth of 2/3 λ_{SAW}) to 2.4μm is quite consistent so that the exciton absorption edges of different QWs coincide at the same photon wavelength. Consequently, a modulator with a 25-QW can be designed to have useful modulator properties. The structure consists of a GaAs substrate, a 2μm $Al_{0.5}Ga_{0.5}As$ lower cladding layer, 25 periods of $Al_{0.3}GaAs/GaAs$ QWs, 1.9μm of $Al_{0.5}Ga_{0.5}As$ of upper cladding layer and a ZnO film on top to enhance the SAW potential. The power of SAW and λ_{SAW} are 10mW and 3μm respectively. Since the core thickness has increased from ~0.14μm in the two previous structures to 0.5μm in the 25-QW structure here, the optical confinement factor of this structure is over 0.92.

The λ_{op} for the absorption modulator should be in the range between 0.859 μm and 0.861 μm. Since all HH exciton peaks of the 25 QWs in the present of the SAW merge with in this wavelength range, a large absorption change can be obtained. Moreover, a negative refractive index change can be achieved in the region between 0.859-0.86μm so that a negative β_{mod}, and thus frequency compression, can be produced, see Fig. 8. The properties of the absorption modulator in this optical wavelength range are given in Table 3. For a SAW aperture of 50μm, β_{mod} and CR are –0.17 and 15.2 dB, respectively for λ_{op} of 0.86μm. For optical modulation, as shown in Fig. 8, variations of the material refractive index change with wavelength is almost the same in comparison to the 5-QW structure where the curves do not coincide as shown in Fig. 5. For a SAW aperture of 50μm, one-tenth of the 5-QW structure, at a selected λ_{op} of 0.870μm, the phase change is > 0.51 radian and η is above 6.3 for a β_{mod} of 10.8. The refractive index change for a bulk AlGaAs SAW modulator is ~10^{-4},[18] while it is ~10^{-3} in our optical modulator, as given in Table 3. This implies that the optical modulation obtained here is an order of magnitude better than a conventional bulk III-V semiconductor SAW device. For both electro-optic and electro-absorption modulators, since the number of QW periods increases to 25, the SAW aperture can be reduced from 500μm to 50μm while the CR retains the same order of magnitude. Therefore, the interaction time between the mode field and the SAW reduces, which implies that the modulator bandwidth also increases in the 25-QW structure.

Table 3. Modulation properties of the 25 QWs modulator. The SAW aperture is 50 μm.

	absorptive modulation				
λ_{op} (μm)	α_{loss} (cm^{-1})	$\Delta\alpha_{eff}$ (cm^{-1})	Δn_{eff} (10^{-2})	CR (dB)	β_{mod}
0.859	644.5	2041	–3.0	10.2	–2.14
0.86	520.5	3029.5	–3.48	15.2	–0.17
0.861	431	2585	1.83	12.9	1.03
	phase modulation							
λ_{op} (μm)	α_{loss} (cm^{-1})	$\Delta\alpha_{eff}$ (cm^{-1})	n_{eff} (SAW)	n_{eff} (no SAW)	$\Delta\phi$ (rad.)	η	l for $\Delta\phi=\pi$	β_{mod}
0.869	162.6	36.1	3.48234	3.48079	0.56	7.64	280	6.2
0.870	149.7	18.9	3.48001	3.47860	0.51	6.34	308	10.8
0.871	138.6	7.1	3.47781	3.47654	0.46	5.15	343	25.8

4. CONCLUSIONS

SAW produce electro-absorptive and electro-optic modulations in QWs have been investigated theoretically. The QW active region including 100Å $Al_{0.3}Ga_{0.7}As$/GaAs single QW, 5 periods QW and 25 periods QW. Since the SAW effects reduce non-uniformly with depth in these structures, the location of the QW stack and its number of period need to be designed and optimized carefully. Our results show that the active QW region with a thickness less than 5% of λ_{SAW} should best be placed at the top surface so that strong SAW effects can be utilized. For a thick QW structure, such as 25 period QW, an uniform SAW induced electric field is required and therefore the period QW should be is located at a depth of ~ 2/3 λ_{SAW} below the top surface where the SAW induced field is of a lower magnitude. Since the SAW potential in this region is small, deposited ZnO films are required to enhance the SAW induced potential. Moreover, longer λ_{SAW} are used to obtain a more linear SAW potential. Optical confinement of the active region is shown to be important for the high modulation efficiency. For modulation with thin active QW region, such as single and five period QW structures, high Al concentration cladding layers should be used.

From the modulation properties of the three QW periods, it is concluded that the single QW structure provides better absorption modulation than the 5-QW structure, while it is opposite for the optical modulation. The 25-QW modulators offer the advantage of a smaller SAW aperture, and thus higher modulation bandwidth can be achieved as compared to the other two smaller QW structures. By comparison with conventional SAW devices, the effective index change of these SAW-QW devices provide at least a 10 times improvement. Consequently, using SAW to produce large electro-optic and electro-absorptive modulators makes the acousto-absorptive and acousto-optic devices much more attractive than the bulk or heterojunction structures for SAW applications.

5. ACKNOWLEDGEMENTS

6. REFERENCES

1   M. Hatori, H. Muira, H. Sunagawa, M. Takeuchi and K. Yamanoushi, "Waveguide type multifrequency acousto-optic modulators", Jpn. J. Appl. Phys., vol. 32 pp. 3467-3470, 1993

2   J. Chang, N. Harada, S. Kashiwa, "High frequency acousto-optic deflector using ZnO thin film deposited on an amorphous substrate", Electron. Lett., vol. 23, pp. 1384-1385, 1987.

3   C. D. Tran and M. Bratelt, "Performance characteristics of an acousto-optic tunable for optical spectrometry", Rev. Sci, Instrum., vol. 63, pp.2932-2939, 1992.

4   Y. Abdelarzek and C. S. Tsai, "An integrated optic RP spectrum analyzer in a ZnO-GaAs-AlGaAs waveguide", J. Lightwave Technol., vol. 8, pp.1833-1839, 1992.

5   T. Gryba, J. E. Lefevra, "Optimization of MQW structures for acousto-optic absorption modulators", IEE Proc.-Optoelectron., vol. 141, pp. 62-64, 1994.

6   D.S. Chemla, T.C. Damen, D.A.B. Miller, A.C. Gossard, and W. Wiegmann, "Electroabsorption by Stark effect on room-temperature excitons in GaAs/GaAlAs multiple quantum well structures," Appl. Phys. Lett., vol. 42, pp. 864,-866, 1983.

7   D. A. B. Miller, D. S. Chemla, T. C. Damen, A. C. Goddard, W. Wiegmann, T. H. Wood, and C. A. Burrus, "Electric field dependence of optical absorption near the band gap of quantum-well structure," Phys. Rev. B. vol. 32, pp. 1043-1060, 1985.

8   T. H. Wood, "Multiple quantum well (MQW) waveguide modulators", J. Ligthwave Technol., vol. 6, pp.743-757, 1988.

9   Y. Kas, H. Nagai, M. Yamaniahi, I. Suemune, "Field efects on the refractive index and absorption coefficient in AlGaAs quantum well structures and their feasibility for electrooptic device applications", IEEE J. Quantum Electron., vol. 23, pp. 2167-2179, 1987.

10   Y. Kim, and W. D. Hunt, "Acoustic fields and velocities for surface-acoustic-wave propagation in multi-layered structures: An extension of the Laguerre polynomial approach", J. Appl. Phys., vol. 68, pp.4993-4997, 1990.

11   C. Thompson, and B. L. Weiss, "Characteristics of surface acoustic wave propagation in III-V semiconductor quantum well structures", J. Appl. Phys., vol. 78, pp. 5002-5007, 1995.

12   A. R. Adams and D.J. Dunstan, "Analysis and design of low-dimensional structures and devices using strain: I. Hydrostatic pressure effects", Semicond. Sci. Techol., vol. 5, pp. 1194-1201, 1990.

13 W. C. H. Choy, B. L. Weiss, and E. H. Li, "The AlGaAs/GaAs quantum well electrooptic phase modulator with disorder delineated optical confinement," IEEE J. of Quantum Electron., January, 1998.

14 W.C.H. Choy, E.H.Li, and J. Micallef, "The polarization insensitive Electro-absorptive and -refractive Modulation by Utilizing InGaAsP/InP interdiffused quantum well," IEEE J. of Quantum Electron. vol. 33, pp. 1316-1323, 1997.

15 W. C. H. Choy, and E. H. Li, "The applications of interdiffused quantum well in normally-on elecro-absorptive Fabry-Perot Reflection Modulation", IEEE J. of Quantum Electron., vol. 33, pp. 382-393, 1997.

16 T. Hausken, R. H. Yan, R. I. Simes, L. A. Coldren, "Relating the chirp parameter to the number of quantum wells in GaAs/AlGaAs waveguide modulators", Appl. Phys. vol. 55, pp.718-720, 1989.

17 Y. Kim and W. D. Hunt, "An analysis of surface acoustic wave propagation in a piezoelectric film over a GaAs/AlGaAs hereostructure", J. Appl. Phys, vol. 71, pp. 2136-2142, 1992.

18 R.G. Hunsperger, Integrated Optics: Theory and Technology, New York: Springer-Verlag, 1985, chp. 9.
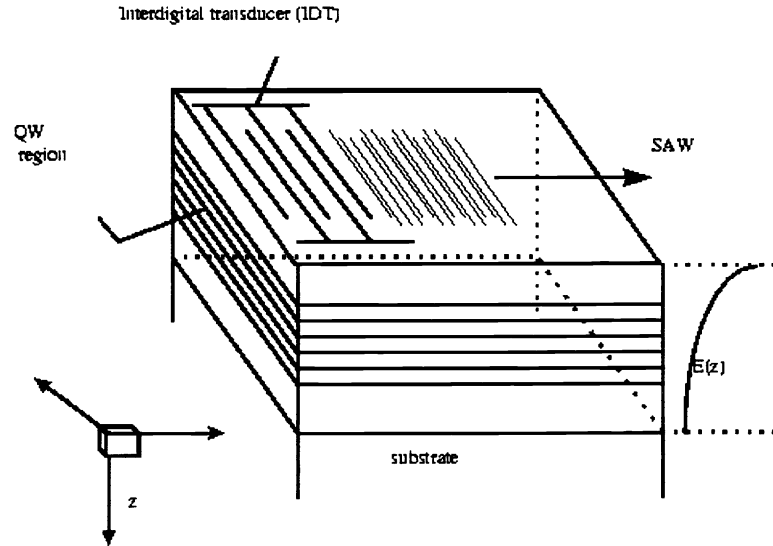
Fig.1 Schematic diagram of the propagation of a SAW on top of QWs structure. E(z) is the SAW induced piezoelectric field amplitude, where z is the direction normal to the plane of the quantum wells.
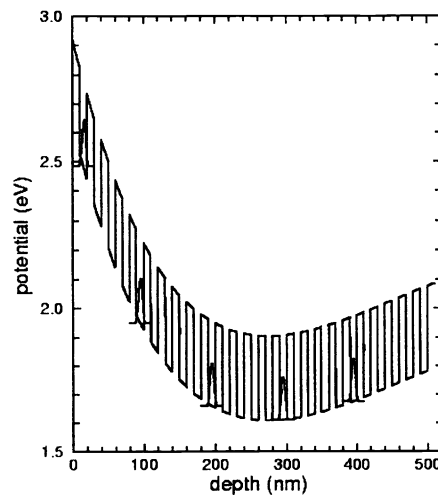

Fig.2 25 periods of QWs on top of $Al_{0.5}Ga_{0.5}As$ cladding tilted by SAW potential. The first wavefunction of the 25 periods of QWs localize in the well without serious tunneling.
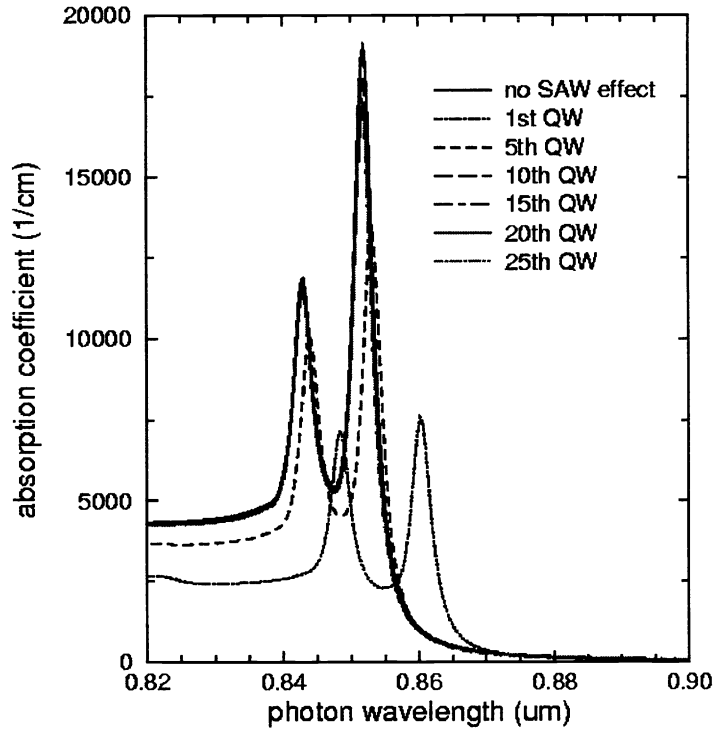
Fig.3   TE mode absorption spectra of 25 periods of QWs on top of $Al_{0.5}Ga_{0.5}As$ cladding, no SAW effect (solid line): 1st QW (dot line), 5th QW (dash line), 10th QW (long dash line), 15th QW (dash-dotted line), 20th QW (light color solid line), 25th QW (light color dot line).
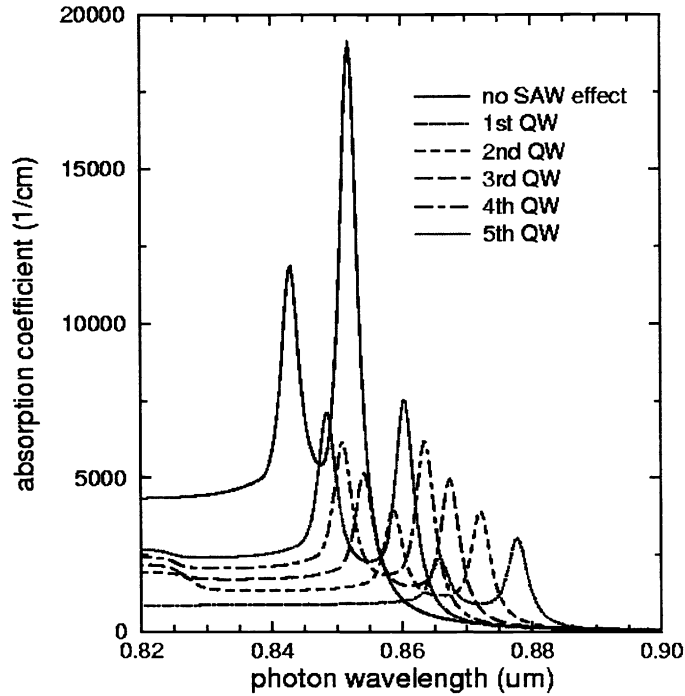

Fig.4   TE mode absorption spectra of QWs in the 5 QWs modulator: QW without SAW effect (solid line), 1st QW (dot line), 2nd QW (dash line), 3rd QW (long dash line), 4th QW (dashed dot line), 5th QW (light color solid line).
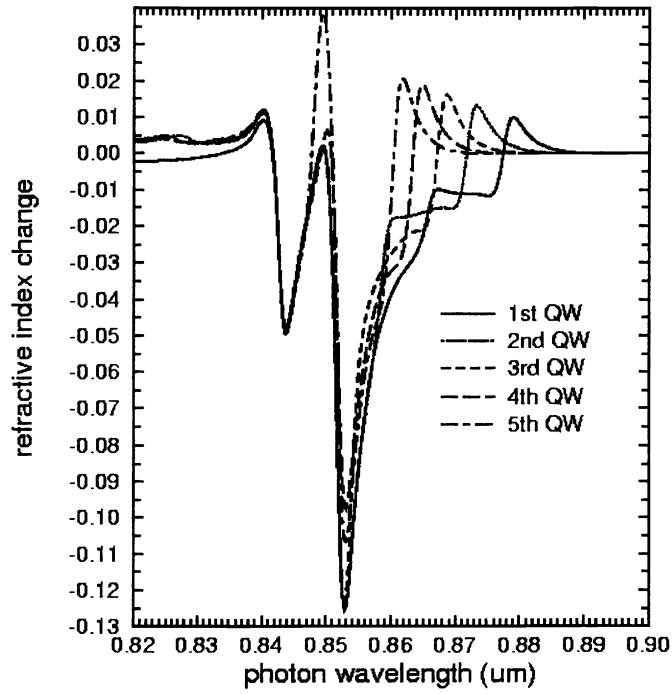
Fig.5 TE mode refractive index spectra of QWs in the 5 QWs modulator: 1st QW (solid line), 2nd QW (dot line), 3rd QW (dash line), 4th QW (long dash line), 5th QW (dashed dot line).
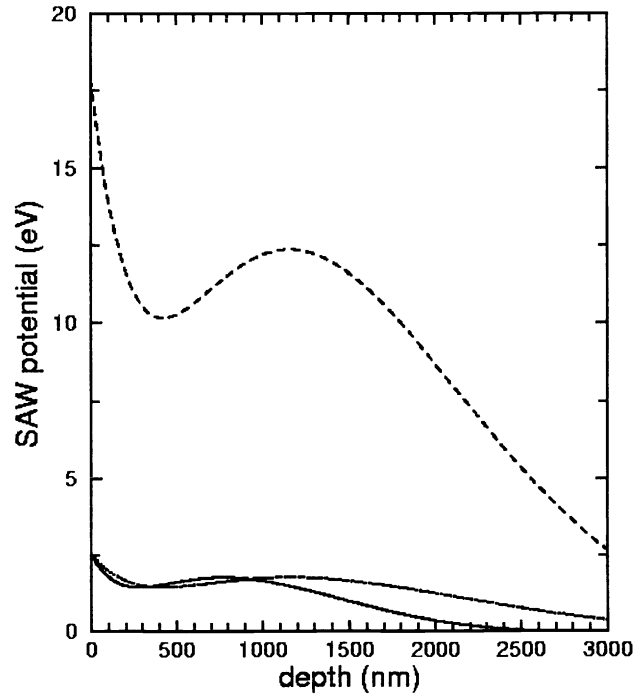

Fig.6 SAW potential in different material structures: 25 QWs located at depth from 1.9 μm to 2.4μm and SAW with 2μm wavelength launched (solid line), the same structure and SAW with 3 μm wavelength launched (dot line), and the same structure with ZnO deposited on top and SAW with 3μm wavelength launched (dash line).
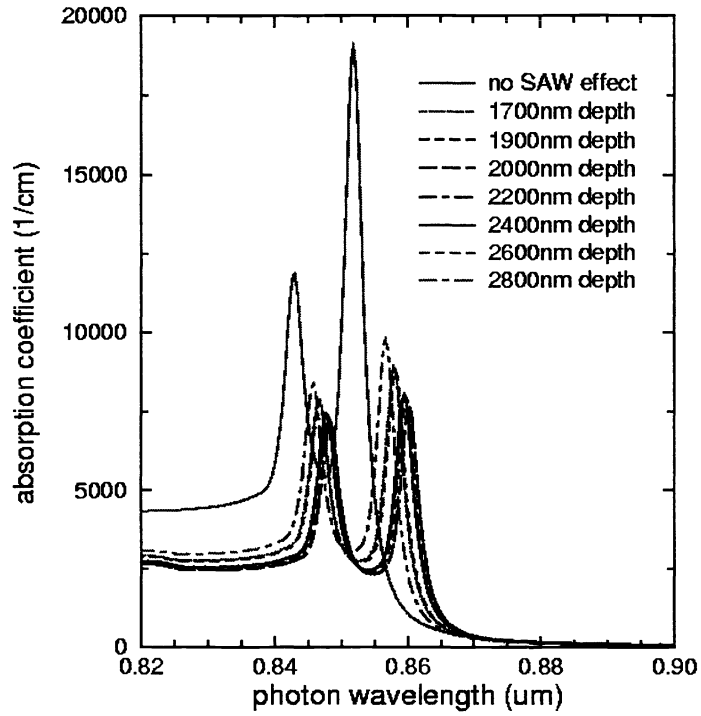
Fig.7 TE mode absorption spectra of a QWs at different depth from 1.7μm to 2.8μm: a reference QW without any SAW effect (light solid line), QW at 1.7μm (light dot line), QW at 1.9 μm (dashed line), QW at 2μm (long dash line), QW at 2.2μm (dashed dot line), QW at 2.4μm (light dash line), and QW at 2.8 μm (light dashed dot line).
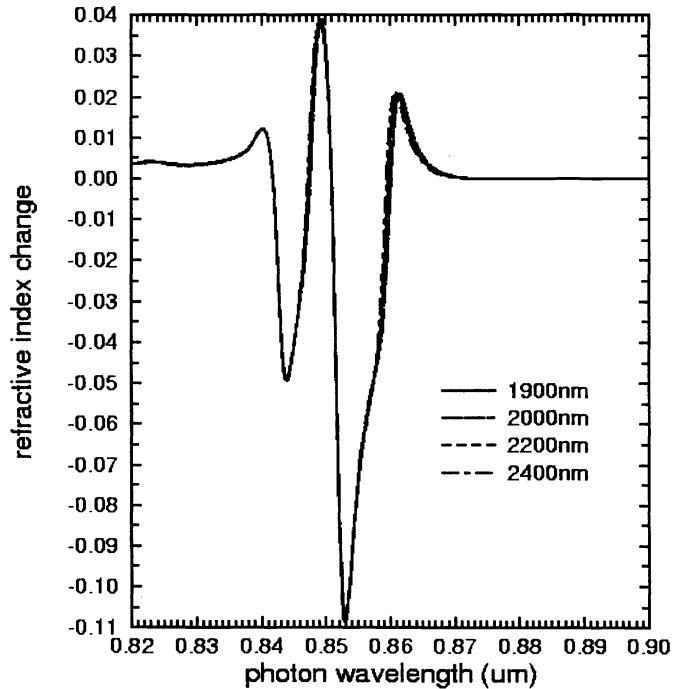

Fig.8 TE mode refractive index spectra of QWs in the 25 QWs modulator: QW at 1.9μm (solid line), QW at 2μm (dot line), QW at 2.2μm (dash line), and QW at 2.4 μm (long dashed line).